Bulletin of Electrochemistry 18 (11) November 2002, pp 489-495 0256-1654/2002/$ 3-50

CYCLIC VOLTAMMETRIC STUDIES ON THE ELECTROCHEMICAL BEHAVIOUR OF CUPRONICKEL IN SODIUM CHLORIDE SOLUTION

J MATHIYARASU, N PALANISWAMY AND V S MURALIDHARAN

Central Electrochemical Research Institute, Karaikudi 630 006, Tamil Nadu. INDIA

[Received: 27 February 2002 Accepted: 04 July 2002]

The electrochemical behaviour of the dissolution of cupronickel in aqueous sodium chloride solutions was investigated through cyclic voltammetric and X-ray diffraction studies. This investigation analyses the discrepancies existing in the ideas related to cupronickel dissolution whether selective dissolution/ simultaneous dissolution. Anodic dissolution of cupronickel alloys is found to be potential dependent. Selective dissolution takes place at lower potentials and simultaneous dissolution at higher potentials. The rate of simultaneous dissolution of the alloy is lower than that of the anodic dissolution of pure copper.

Keywords: Cupronickel and X-ray diffraction.

INTRODUCTION

Cupronickels are being extensively employed in marine environments because of their excellent corrosion and biofouling resistance. Over the few decades, the use of these alloys was extended to ship hulls, mesh for fish cages, cathodic protection, antifouling anodes and intake screens at power stations [1]. The electrochemical behaviour has been studied in different aqueous solutions using different techniques [2-5]. There is no agreement on the mode of dissolution of these alloys in pure chloride solutions and the results are be set with a number of discrepancies.

Two mechanisms are in vogue on the mode of dissolution of Cupronickels based on previous investigations: a). the selective dissolution of one of the elements from the crystal lattice leaving a porous matrix, b) the simultaneous dissolution of both the components of the alloy followed by redeposition of one of the components on the surface. Contradictory results were also reported in sodium chloride solutions. Some authors proposed the predominant selective dissolution of nickel [6] while others suggested dealloying as a result of dissolution of copper [7-8]. Efird [9] was of the view that cupronickels are immune to dealloying in seawater at potentials more negative than -200 mV (SCE) at pH < 8.5 for 90 Cu-10 Ni and < 7.8 for 70 Cu-30 Ni.

This paper reports the dissolution behaviour of cupronickel alloys (Ni-10-30%) in neutral sodium chloride solutions. Attempts are also made to find out the pattern of dissolution of these alloys in neutral chloride media using voltammetry and X-ray diffraction techniques.

EXPERIMENTAL

High purity copper (99.99%) and nickel (99.99%) and three cupronickel alloys of increasing nickel content were used as the working electrode. The composition of these alloys is given in Table I.

The working electrodes were made into a cylindrical rod having an area of cross section of

TABLE I: Composition of cupronickels used

Alloy	Cu (%)	Ni (%)
I	87.29	12.70
II	76.39	23.61
III	67.66	32.34

0.385 cm^2. The rods were embedded in Teflon gaskets so that only the cross-sectional surface of each electrode was in contact with the solution. A platinum foil and a saturated calomel electrode (SCE) served as counter and reference electrode respectively. Potential in the text refers to the SCE scale. Measurements were made in neutral sodium chloride solutions of varying concentrations ranging from 0.025 to 0.5 *M* The specimens were mechanically polished using 4/0 emery paper and the solutions were oxygenated by bubbling purified oxygen for an hour before the experiment.

Cyclic voltammetric measurements were carried out using a Potentiostat (EG&G 173), Universal programmer (EG&G 175) and the E/i data recorded with X-Y recorder (Rikadenki 201T). All measurements were carried out at 298 ± 0.5 K. The surface layer was analysed by using a computer controlled X-ray diffractometer (JEOL JDX 8030) with CuK_α (Ni filtered) radiation (λ = 1.5418 A^0) at a rating of 40 kV, 20 mA. The scan rate was 0.05-20^0 per step and the measuring time was 1 s/step.

RESULTS AND DISCUSSION

The typical cyclic voltammogram of pure nickel in 0.5 *M* NaCl solution is given in Fig. 1. The curves were recorded between -900 and +500 mV at sweep rates (v) varying from 5 to 100 mVs^{-1}. The anodic current started increasing beyond -100 mV and on the reverse scan, zero current crossing potential (ZCCP) appeared at +200mV. The sweep rate had no influence on the shape of the spectrum excepting a decrease in the current with sweep rate. A broad anodic peak appeared at +300 mV (pseudocapacitative in nature) and no cathodic peak was observed in the reverse scan.

Fig. 2 shows the cyclic voltammogram of pure copper in 0.5 *M* NaCl solution. The electrode was swept between -1000 mV and +700 mV at scan rates varying between 5 and 100 mVs^{-1}. Starting from the zero current crossing potential a very small, probably non-Faradaic current flows upto a certain critical potential above which the dissolution current increases linearly with the applied potential, forming an active region. This is followed by an anodic peak (I_a) followed by

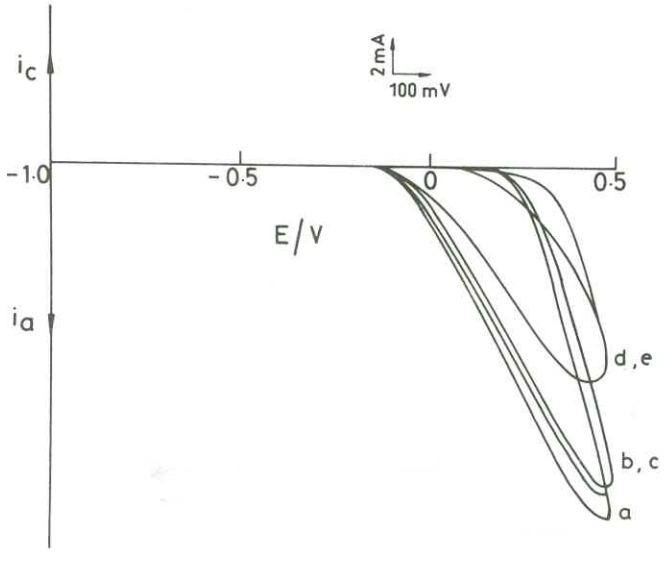

Fig. 1: Cyclic voltammogram of pure nickel in 0.5 *M* NaCl at different sweep rates
a) 5 mV/s b)10 mV/s c) 20 mV/s d) 50 mV/s e) 100 mV/s

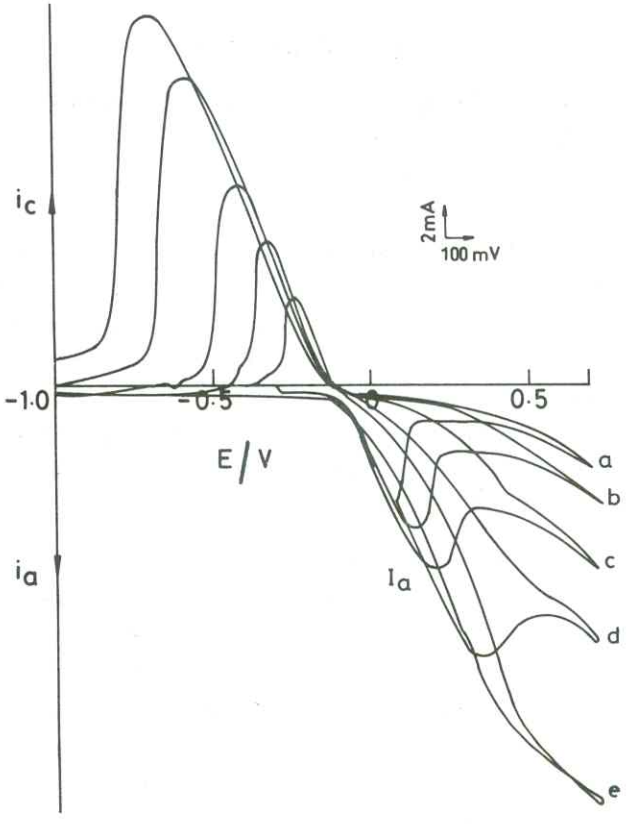

Fig. 2: Cyclic voltammogram of pure copper in 0.5 *M* NaCl at different sweep rates
a) 5 mV/s b)10 mV/s c) 20 mV/s d) 50 mV/s e) 100 mV/s

oxygen evolution. In this region I_a, copper dissolves anodically as follows [10],

$$Cu + 2Cl^- \longrightarrow CuCl_2^- + e \quad (1)$$

There is an increase in the surface concentration of $CuCl_2^-$ ions that undergo hydrolysis [11] to produce a Cu_2O film and thus appear as a peak I_a.

$$CuCl_2^- + H_2O \longrightarrow Cu_2O + 4Cl^- + 2H^+ \quad (2)$$

The formation of solid phase CuCl can also occur [12-13] on the surface within the potential range of peak I_a.

$$Cu + Cl^- \longrightarrow CuCl + e^- \quad (3)$$

The structure of the anodic layer may be represented by an inner layer Cu_2O non-homogeneously covered by CuCl.

When the surface is fully covered with insoluble species, the current decreases to Ipass (passivation current), indicating the formation of a poorly passivating layer. XRD data (Table II) confirm the existence of a mixture of Cu_2O and CuCl on the surface of the electrode potentiodynamically polarised upto +700 mV with a scan rate of 20 mVs^{-1} in 0.5 *M* NaCl solution.

TABLE II: X-ray diffraction analysis of the surface film formed on the Cu/Ni alloy surface

Material	Compound	d-spacings on file A^0	Measured d-Spacings A^0
Copper	Cu_2O	2.47	2.461
		2.14	2.132
		1.51	1.492
	CuCl	3.13	3.092
		1.92	1.862
		1.63	1.598
Cupronickel (90/10)	Cu_2O	2.47	2.446
		2.14	2.120
		1.51	1.464
	CuCl	3.13	3.086
		1.92	1.872
		1.63	1.623
	CuO	2.52	2.620
		2.32	2.331
		2.53	2.537
	NiO	2.09	2.065
		2.41	2.384
		1.48	1.464

The reverse scan exhibits a cathodic peak and the peak corresponds to the electroreduction of Cu^+ to Cu [14]. An increase in the scan rate enhances the peak current (i_p) and shifts the peak potential (E_p) to a more negative value.

Fig. 3 shows the typical cyclic voltammograms of different cupronickel alloys in 0.5 *M* NaCl solution at a scan rate of 5 mVs^{-1}, between -1000 mV and +700 mV. Except for alloy III, the forward voltammogram of alloys I and II exhibit two anodic peaks I_a and II_a. The first peak I_a is due to the formation of Cu_2O and the peak II_a may be assigned to the formation of $CuO/Cu(OH)_2$ [15].

In the case of alloy III, the two anodic peaks coalesce with each other and appear as a single anodic peak. It was assigned to the nickel inclusion that probably increases the ionic and electronic resistivity of the surface layer [3-5]. Hence, further oxidation of Cu_2O to $CuO/Cu(OH)_2$ was suppressed.

On reversing the scan, an inverted anodic peak was observed in the voltammogram (Fig. 3). The appearance of the inverted anodic peak suggests predominant dissolution of the alloy through the pores of the passive film. These peaks are absent for the alloy III, as the surface film was

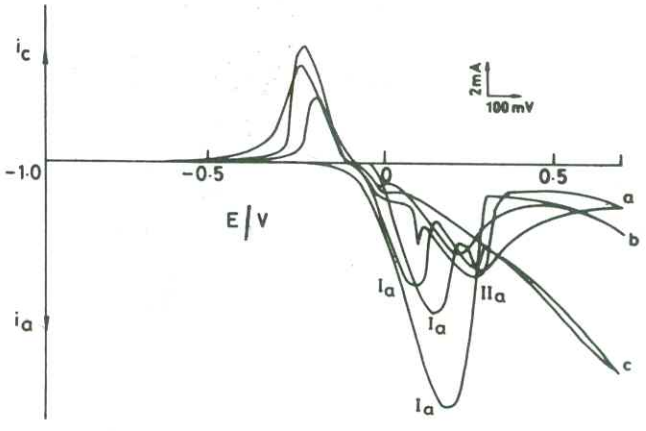

Fig. 3: Cyclic voltammogram of experimental alloys in 0.5 *M* NaCl at scan rate 5 mV/s
a) alloy I b) alloy II c) alloy III

incorporated with nickel resulting in a compact and coherent film.

Increase in the nickel content in the alloy shifts the anodic peak to more nobler values. The slopes of the linear lines in the voltammograms of the alloys do not coincide with that of pure copper. This behaviour could be attributed to the simultaneous dissolution of copper and nickel.

The occurrence of the split anodic peaks indicates supression in the dissolution rate of copper in alloy when compared to that of pure copper. This suppression is due to the dissolution process limited by the inclusion of nickel in the alloy/solution interface. It is evident that the extent of this layer becomes appreciable when the critical potential of dissolution of the alloy is reached. This may explain the decrease in the critical current with the applied potential. This current increases with nickel content in the alloy.

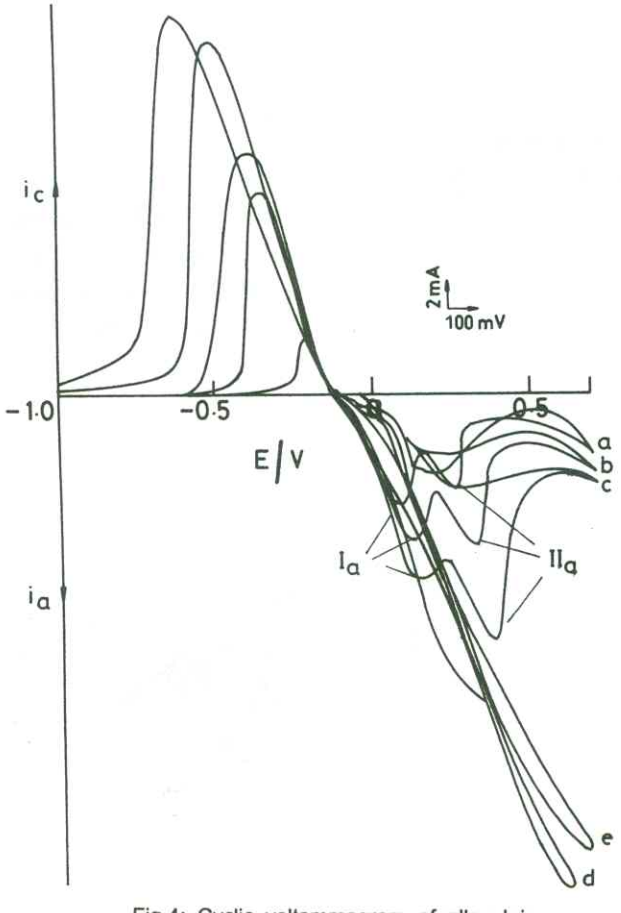

Fig.4: Cyclic voltammogram of alloy I in 0.5 *M* NaCl at different sweep rates
a) 5 mV/s b)10 mV/s c) 20 mV/s d) 50 mV/s e) 100 mV/s

The data reveal that the critical potentials of the alloys are nobler than that of pure copper. This is due to a decrease in the activity of copper atoms through alloying with nickel.

The peak currents (i_p) of peak I_a and II_a and i_{pass} are higher than that of pure copper under identical conditions. The peak potentials (E_p) of I_a and II_a are nobler than that of pure copper. The separation between peak I_a and II_a becomes less and the peak merge with the increase in nickel content. This may be considered to be due to the inclusion of nickel in the surface film. X-ray diffraction studies of these alloys also confirm the existence of Cu_2O, CuCl, CuO and NiO in the surface layer (Table II).

The reverse sweep for these alloys shows a distinct cathodic peak. The broader and more prominent peak is ascribed to the electroreduction of both cuprous and cupric species to copper metal.

The influence of sweep rate on the cyclic voltammetric behaviour of alloy I in 0.5 *M* NaCl is shown in Fig. 4. Similar voltammograms are recorded for the other alloys and the data imply

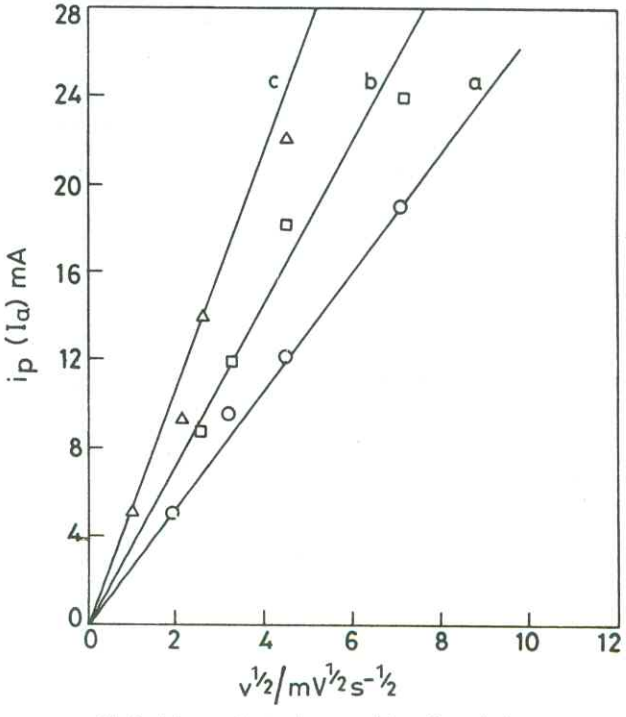

Fig.5: Linear dependence of i_p of peak I_a on $v^{1/2}$ for alloy I to III in 0.5 *M* NaCl
a) alloy I b) alloy II c) alloy III

that an increase in the scan rate enhances I_p of the anodic peaks as well as I_{pass}. The two separated anodic peaks merge and results in a single peak at very high sweep rates. The anodic peak potentials are shifted to more noble potentials and the development of inverted anodic peaks decrease with scan rate. In an analogous manner, i_p of cathodic peak increases and peak potentials shift to more negative values as the sweep rate increases.

In the present study, the effect of scan rate (ν) on I_p and E_p of the anodic peak (I_a) has been quantitatively analysed. Fig. 5 shows the relationship between I_p and $\nu^{1/2}$ for the different alloys in 0.5 *M* NaCl solution. The plots are linear passing through origin. The relationship between i_p (II_a) and $\nu^{1/2}$ was plotted (Fig. 6) and the extrapolated results were different from zero. It was also found that E_p values for anodic peaks (I_a) showed a linear variation with logarithmic scan rate (Fig. 7). These suggest that the anodic process in the two anodic peak ranges are under diffusion control.

The peak current I_p (Ia) is related to the scan rate by,

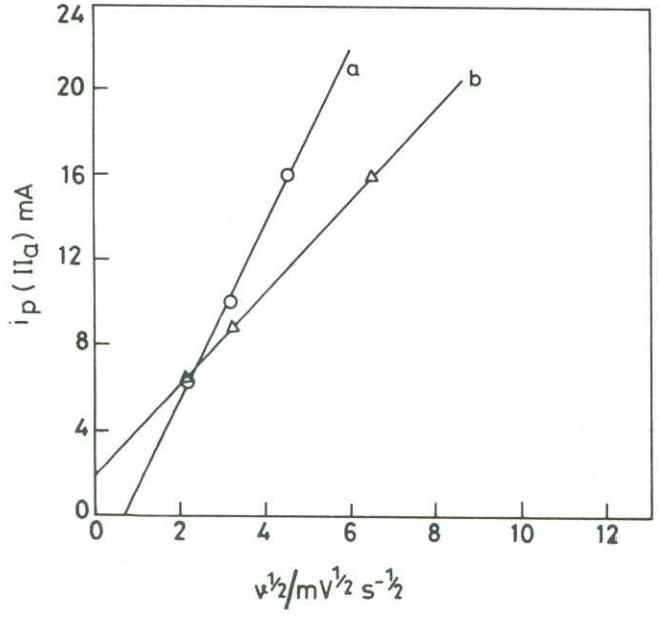

Fig. 6: Linear dependence of i_p of peak IIa on $\nu^{1/2}$ for alloy I to III in 0.5 *M* NaCl
a) alloy I b) alloy II

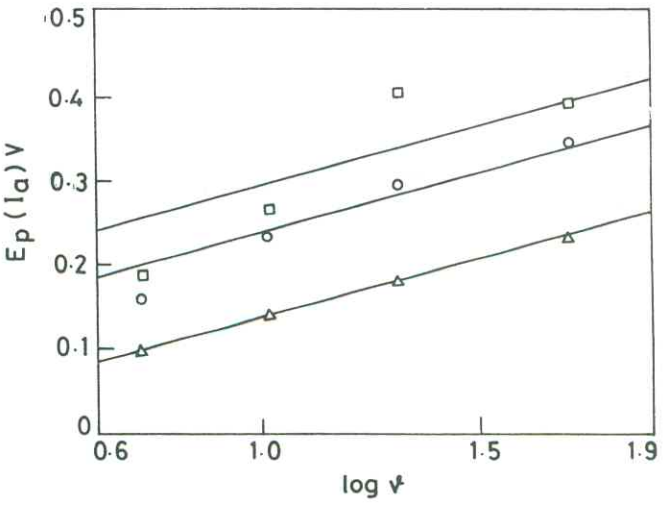

Fig.7: Relationship between E_p and log ν for given alloys I to III in 0.5 *M* NaCl
a) alloy I b) alloy II c) alloy III

$$I_p\ (I_a) \longrightarrow a\,b\,C\,z^{3/2}\,D^{1/2}\,\nu^{1/2} \qquad (4)$$

where a and b are constants, D is the diffusion coefficient of the diffusive species, C is the concentration of the diffusive species, z is the number of exchanged electrons and ν is the scan rate [16].

The effect of concentration of NaCl on the cyclic voltammetric behaviour of alloy I & III is shown in Figs. 8 and 9. Inspection of the results revealed that the peak heights of peak I_a decrease noticeably and at a critical chloride concentration the peak disappears. Their peak potentials shift to

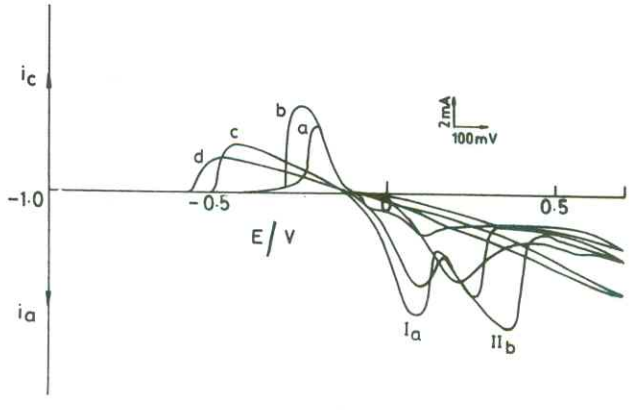

Fig.8: Cyclic voltammogram of alloy I obtained at scan rate 5 mV/s and at given NaCl concentrations in 0.5 *M* NaCl at different sweep rates
a) 0.5 *M* b) 0.25 *M* c) 0.05 *M* d) 0.025 *M*

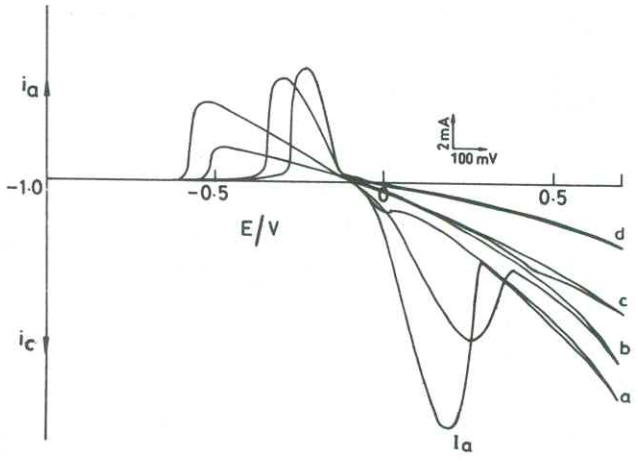

Fig.9: Cyclic voltammogram of alloy III obtained at scan rate 5 mV/s and at given NaCl concentrations in 0.5 *M* NaCl at different sweep rates
a) 0.5 *M* b) 0.25 *M* c) 0.05 *M* d) 0.025 *M*

more negative values with increasing C_{NaCl}. On the other hand, increasing C_{NaCl} slightly decreases I_p (II_a) eventhough its E_p shifts to the negative direction. The passivation current, i_{pass} increases as C_{NaCl} increases. These indicate that the Cu_2O formation occurs through the intermediate formation of $CuCl_2^-$.

The acceleration of dissolution by chloride ions may be due to its direct participation in the elementary act of ionisation of the two metals and to its aggressive action on insoluble products. Plots of log ip against log C_{NaCl} for alloy I and III are given in Fig. 10, where straight lines were observed with that representing the peak I_a, region between 0.5 and 0.025 *M* having a slope very close to 0.8.

The cyclic voltammetric behaviour of these alloys was studied in deaerated 0.5 *M* NaCl solution in order to know the role of dissolved oxygen (Fig. 11). There were no significant differences in the peak current for the anodic and cathodic peaks between the deoxygenated and oxygenated systems (Fig. 3). However, the peak potentials were shifted to more positive side in the absence of oxygen. The presence of oxygen favours the passivation of cupronickels in chloride environment. The hydrolysis reaction is enhanced because of the availability of oxygen [17],

$$4CuCl_2^- + H_2O + \frac{1}{2}O_2 \longrightarrow 2Cu_2O + 8Cl^- + 2H^+ \qquad (5)$$

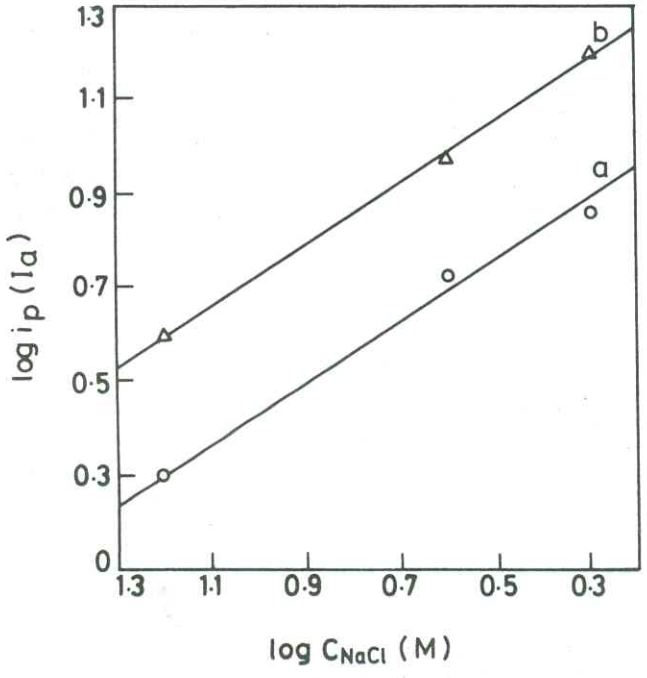

Fig. 10: Linear dependence of log i_p (I_a) against log C_{NaCl} for alloys at scan rate 5 mV/s
a) alloy I b) alloy III

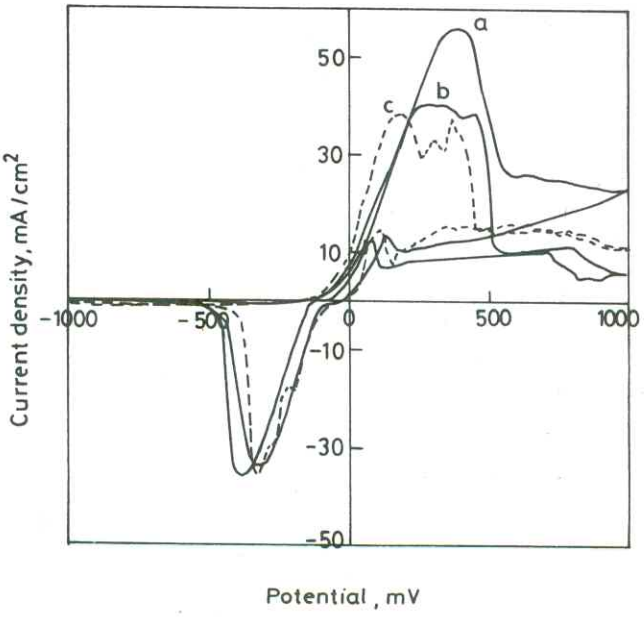

Fig.11: Cyclic voltammogram of given alloys at scan rate 5 mV/s in deaerated 0.5 *M* NaCl solution
a) alloy I b) alloy II c) alloy III

The hypothesised reaction can explain the shift in the i_{pass} to the noble direction. This reaction supports the thinner, apparently more protective corrosion product film.

CONCLUSION

The electrochemical behaviour of cupronickel alloys in sodium chloride solution was studied using cyclic voltammetry and X-ray diffraction measurements.

Anodic dissolution of these alloys was found to be potential- dependent as the curves display two well defined potential regions. Preferential dissolution of copper component is observed in the first one whereas both copper and nickel dissolve simultaneously in the second.

The passivation is due to the formation of duplex film consisting of inner compact Cu_2O layer. The Cu_2O formation was found to be through $CuCl_2^-$ intermediate formation. The rate of dissolution increases with sodium chloride concentration and scan rate.

The dissolved oxygen enhances the passivation of cupronickels, which results in shifting of the I_{pass} in the nobler direction. Increase in the oxygen concentration favours the cathodic reaction whereas the decrease in oxygen concentration favours alloy dissolution.

The rate of simultaneous dissolution of the alloy is lower than that of anodic dissolution of pure copper under identical conditions. The rate of simultaneous dissolution decreases with the nickel content in the alloy matrix. The presence of NiO in the defective copper oxide passive layer improves the film stability of the film.

REFERENCES

1. A H L Chamberlain and B J Garner, *Biofouling,* **1** (1988) 79
2. M E Walton and P A Brook, *Corros Sci,* **17** (1977) 317
3. R F North and M J Pryor, *Corros Sci,* **10** (1970) 297
4. H P Dhar, R E White, R Darby, L R Cornwell, R B Griffin and G Burnwell, *Corrosion,* **41** (1985) 193
5. H P Dhar, R E White, G Burnwell, L R Cornwell, R B Griffin and R Darby, *Corrosion,* **41** (1985) 317
6. R G Blundy and M J Pryor, *Corros Sci,* **12** (1972) 65
7. W B Brooks, *Corrosion,* **24** (1968) 171
8. S Petetin, J Crousier and J P Crousier, *Mater Chem Phys,* **10** (1984) 317
9. K D Efird, *Corrosion,* **31** (1975) 77
10. C I Elsner, R C Salvarezza and A J Arvia, *Electrochim Acta,* **33** (1988) 1735
11. A J Bacarella and J C Griess, *J Electrochem Soc,* **120** (1973) 461
12. L Brossard, *Corrosion,* **40** (1984) 420
13. M Metikos-Hukovic and I Milosev, *J Appl Electrochem,* **22** (1992) 448
14. A M Shams El Dim and F M Abdel Wahab, *Electrochim Acta,* **9** (1964) 113
15. H H Strehblow and B Titze, *Electrochim Acta,* **25** (1980) 839
16. P Delahay, *'New instrumental methods in Electrochemistry',* Wiley- Interscience, New York (1954) 124
17. H H Lu and D J Duquette, *Corrosion,* **46** (1990) 843